Determination of the transition threshold from laminar flat flames to turbulent flames by a CO_2 laser irradiation method

June Sung Park, Osamu Fujita*, Yoshikazu Taniyama
Hokkaido University
Sapporo, Hokkaido, Jappan

1 Introduction

The flame propagation in a tube has been investigated intensively by many researchers, because of its practical importance in different types of combustion devices. As fundamental aspects of propagating flames, the shapes of flame fronts investigated could display the most reliable features to provide a general insight into combustion waves. There are a number of inherent instability modes in premixed flames [1]. Diffusive-thermal instability, initiated by unequal diffusion of reactant and heat (Le<1), may occur when the flame curvature is comparable to the flame thickness. Hydrodynamic instability was first recognized by Darrius in 1938 [2]. When the flame front is wrinkled with moderate amplitude, the flow of unburned mixture in front of the flame surface undergoes divergence and convergence at convex and concave states of the flame front, respectively. This was experimentally identified by Clanet and Searby in 1998 [3].

Acoustic influences on combustion systems are also important to understand the dynamic behaviors of flame fronts in a combustion tube. The general theory of acoustic instability was established by Rayleigh in 1878 [4]. It was shown that if changes in heat release are in phase with the acoustic waves, acoustic oscillation will be enhanced cycle by cycle.

In a classical study of the acoustic instability in a tube [5], Serby reported distinct regimes of unstable flame behaviors. These can be categorized into: (1) A curved shape with a large cell, just after ignition. Overall the flame speed is twice its laminar burning velocity due to the increased flame area. At this moment, the acoustic amplitude (acoustic velocity) increases significantly increasing the total flame area. (2) Primary acoustic instability with a flat flame surface. It features an almost planar flame front. After regime (1), the primary acoustic instability is formed with a relatively stable level of acoustic pressure. (3) A violent secondary acoustic instability with a sudden formation of cellular structures on the flame surface. (4) Turbulent motion. As a detailed investigation of the above observations [6], Searby and Rochwerger developed theoretical predictions through stability diagrams in terms of wave numbers and acoustic intensities, and have verified the stability diagrams with experimental data. They used a loudspeaker at the bottom, producing a stable planar flame that was classified as the primary acoustic instability in [5]. Then, the threshold of the parametric instability leading to the turbulent motion of the flame front was given as a function of the frequency and flame surface`s wave number of the imposed acoustic field by using the loud spearker. In a theoretic study of the acoustic instability Pelce and Rochwerger [7] investigated the position of occurrence of the primary acoustic

Correspondence to: ofujita@eng.hokudai.ac.jp

instability by predicting the growth rate of the acoustic pressure. The analysis was limited to small amplitudes of cellular flames. Both researches [6, 7] considered only small amplitudes of the flame front waves as the interface of two different densities. In some cases, the amplitude of the flame front, however, changes very much, which could be a further factor to control the transition process in actual flames.

This study attempts to establish and observe the transient process to the parametric instability with the sudden increase of flame surface area. We initially form a flat flame as a default state [8]. Then, CO_2 laser light is irradiated normal to the flat flame [8]. The laser irradiation into the unburned mixture deforms the flame shape, resulting in a sudden increase in the flame surface area. The shape of the deformed flame is strongly dependent on the laser power and beam diameter, which allows the generation of a desired flame wave number and wave amplitude of the flame structure. The object of this paper is to establish criteria for transition from the primary to the secondary instability in terms of laser power and to investigate how the flame configuration arising from the laser light absorption affects the onset of the secondary instability.

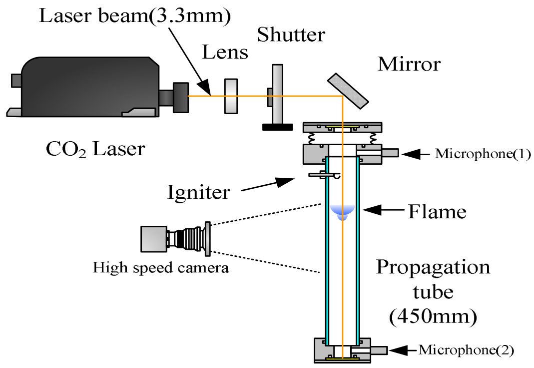

Figure 1 Schematic outline of the experimental setup.

2 Experimental setup

The experimental apparatus is schematically outlined in Fig. 1. The propagation tube (transparent acrylic tube, 45.0 cm long, and 5.0 cm inner diameter) is set vertically and is filled with the tested gas (Table 1) at atmospheric pressure. Ethylene gas was used as it is the main absorption medium of CO_2 laser light according to the NIST chemical database [9]. Carbon dioxide was selected as an inert gas to reduce the burning velocity. Since the Lewis number ($Le=a/D_{o2}$, a: thermal diffusivity of the mixture, D_{o2} :mass diffusivity of the insufficient component) is less than unity, the flame front may be unstable with some disturbance on the flame surface. In the experimental arrangement here, there is an automatic opening device powered by an electro-magnet and a mechanical spring at the upper end of the tube. When the spark igniter is activated, the exhaust part is simultaneously opened. The premixed gas inside the tube is continuously exposed to the laser beam (beam diameter 3.3mm, SYNRAD Firester v20, wavelength 10.6 μm) from 0.8 seconds after activating the igniter, and the CO_2 laser beam preheats the unburned mixture at the center. A mechanical shutter is set in the laser path to control the exposure timing of the laser beam. The motion of the flame fronts is captured by a high speed camera (3200 fps). The moment of laser irradiation is defined as t = 0 ms. Two microphones (Onosokki M1432) are placed one near the open end and one at the bottom end to observe the sound pressure fluctuations (data sampling rate, 10k Hz).

3 Result and discussion

3.1 Dynamic motion of flame front

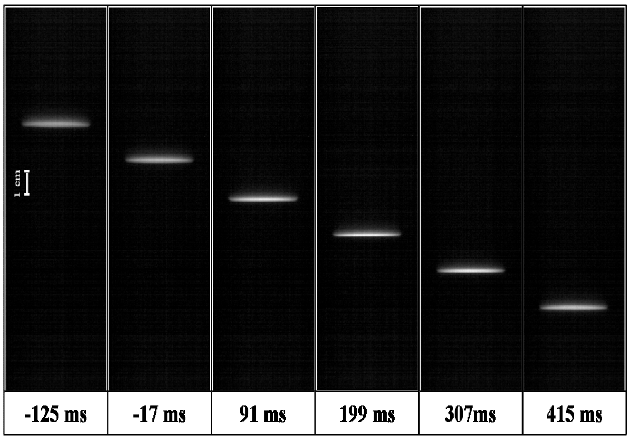

Figure 2. Still images of the temporal evolution of flame fronts without laser power.

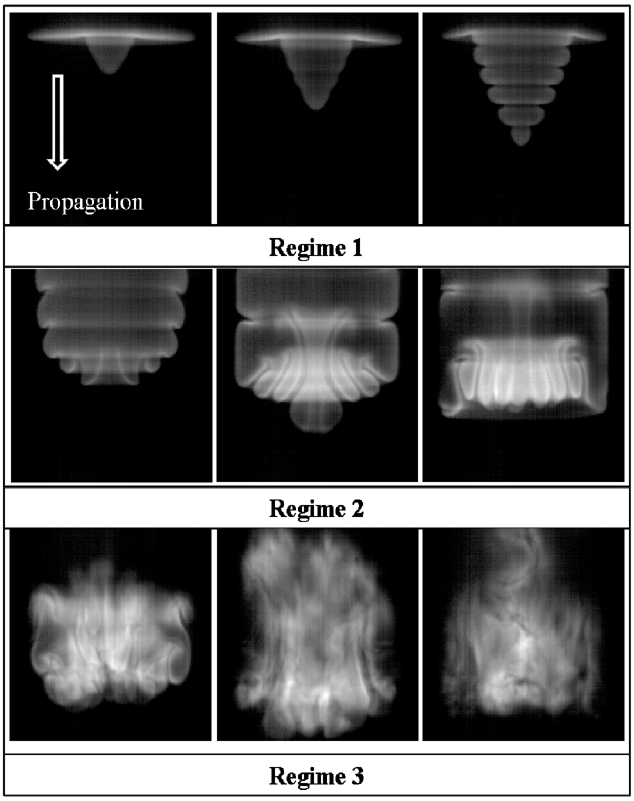

Figure 3. Figure 3. Still images of flame shapes with a laser power of 18W.

To be able to observe the transition process to turbulent motion initiated by flame front distortion by CO_2 laser absorption clearly, it is desirable to have a completely flat flame prior to the laser irradiation, as a default flame. Upon ignition, a large soft flame front propagates downward due to hydrodynamic instability. And then, the flame front rapidly becomes flat at the upper part of the tube. Figure 2 shows a downward propagating flat flame in the combustion tube without laser power application, this is the primary acoustic instability state in Ref. [5]. Once the flat flame is established in the tube, the flat surface is maintained during the propagation. In the experiments the propagating flame is irradiated with the CO2 laser beam as described in Fig. 2. Then, the ethylene in the unburned mixture absorbs the laser energy just ahead of the flame surface along the center axis. The local flame velocity of the preheated unburned mixture increases and distortion of local flame shape occurs. In cases of low laser power, below a critical value, there is no transition process as discussed below although we do not present the data here.

Figure 3 shows the typical behaviors of a propagating flame after the laser irradiation with *Le*<1 mixture as used in this study. When the flame front has a positive curvature, it is exposed to diffusive-thermal effects increasing the flame tip velocity in addition to the effect of local heating by the laser light absorption. Thus, the flame tip shows unstable behaviors in regime 1 in Fig. 3. Details of the flame characteristics in regime 1 can be found in Ref. [8]. Then in regime 2, the corrugated flame front structure appears as seen in the figure. This corresponds to the secondary acoustic instability noted in Refs [5, 6]. Finally in regime 3, the flame front shows strong turbulent motion with breaking up of its cellular structures and explosive acceleration of the flame front. Figure 4 depicts (a) temporal variations of the flame tip position, (b) the flame tip velocity with a laser power of 8W and (c) the velocity with 18W of laser power. For the laser power of 0W, the flat flame front propagates to the bottom of the tube with constant average velocity accompanied by periodic back and forth motion. The slope of the flame tip position after 95 ms increases when there is absorption of laser light. The initiation of laser irradiation is at 0 ms, and around 95 ms of induction time appears to elapse before the local acceleration takes place. Figure 4 shows that strong acceleration of the flame tip position and a gradual increase in the periodic motion appears in regime 1 for both the cases of 8W and 18W laser light irradiation. Diffusive-thermal effects and acoustic influences may be the main causes of this acceleration. In regime 2, there is a sudden decrease in the amplitude of the flame tip velocity fluactuation followed by a gradual increase to the total area of the flame front to equal that in regime 1 finally, this is the secondary acoustic instability.

3.2 Thresholds of transition

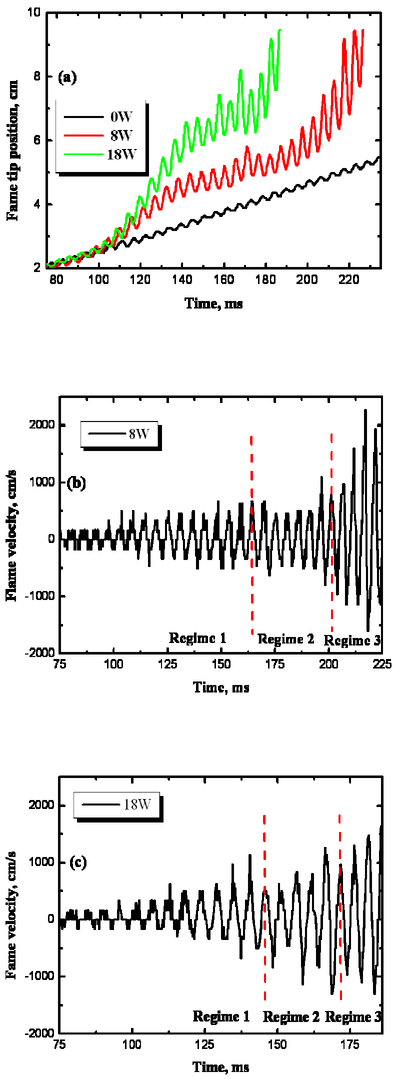

Figure 4. (a) Temporal variations in the flame tip position, and (b) flame tip velocity with a laser power of 8W, and (c) 18W.

Practically, the combustion processes in most combustion devices encounter energy feedback of the reaction zone into the acoustic field. Thus, detailed information of the thresholds of the parametric instability must be provided to more fully understand these explosive transitions. Figure 5 shows definition of the moment when the flame tip curvature changes from convex to concave. When the Lewis number is less than unity and the curvature is positive, acceleration of flame tip additional to that provided by the laser absorption effect is induced. Therefore, the structure of Fig. 5 is not attained without acoustic field. With the presence of acoustic fluactuations, the negative curvature as seen in Fig. 5 may be attained by a positive pressure gradient. In a positive pressure gradient along the tube axis, the curved flame tip becomes filled with low density burned gas which is selectively accelerated to the open end of tube and it changes to the concave structure. Here we wish to define the transition time to the secondary instability as the time to attain the situation of Fig.5 from the moment of ignition, because once a structure like that in Fig. 5 is attained during the propagation, the corrugated structure and following explosive turbulent phenomena occur imediately. Based on the experiments reported above, we measured the transition time to the secondary instability based on the definition above with various laser power inputs.

Figure 6 depicts the transition time (time to attain the structure of Fig. 5 from time of ignition) with various laser powers, limited to the laser powers from 8 to 18W where the transition phnomena are observed. In Fig. 6, the transition time decreases with increasing laser power to a minimum value at 12W. In the case of a laser power of 8W, deformation of the flame tip is the smallest in the tested range. Nevertheless, the increased surface area at 8W provides feed back of thermal energy to the acoustic field in the tube and it satisfies the Rayleigh criterion [4]. Then, it goes on to the transition to the secondary instability condition with a given delay time as seen in Fig. 6. when the laser power increases to 12W, the growth rate of the flame surface area becomes faster and the time to reach the secondary instability becomes shorter.

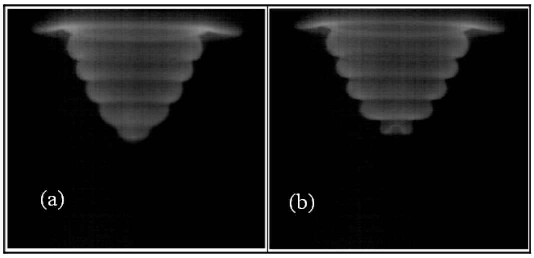

Figure 5. Definition of the moment of transition To the secondary acoustic instability. (a) last moment of regime 1, (b) initiation of the secondary instability.

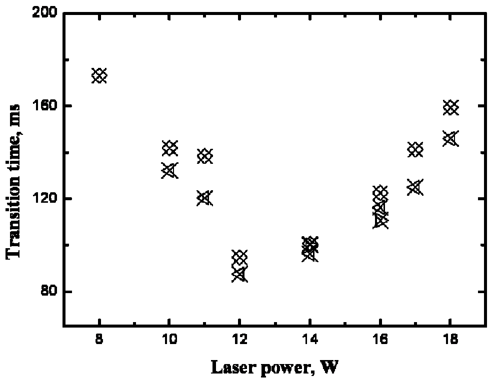

Figure 6 The transition times with various laser powers, as defined in this study.

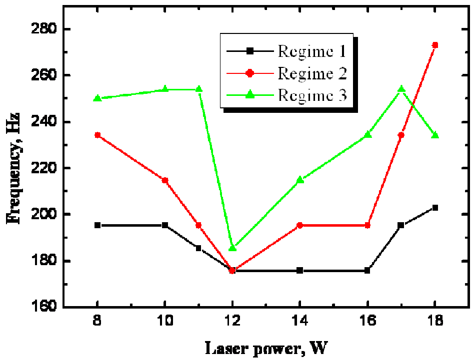

Figure 7. Masured acoustic frequencies.

After the minimum transition time at 12W in Fig. 6, the time to the transition increases as the laser power increases. This may be explained by the non-linear increase in the local flame velocity with the increase in premixed gas temperature with the very strong laser power (also see Fig. 8). The non-linear increased flame velocity overcomes the effect of the positive pressure gradient for a longer period even with the faster growth rate of the surface area.

For a futher understanding, the measured acoustic frequency at each regime was determined as a function of supplied laser power and the results are shown in Fig. 7. The changes in acoustic frequencies suggested by Fig.7 are consistent with Fig. 6. For the 8W laer power, the measured frequency increases with time (increasing regime number). The tube used in the experiment was excited at the 1/4 wavelength longitudinal mode. The acoustic frequency(f), $f=c/4L$, increases due to the increases in sound speed(c) as the flame front aproaches the closed end of tube. Therefore the earlier regime results in a lower acoustic frequency. In figure 7, the acoustic frequency at regime 2 decreases at laser powers less than 12W. This is because the transition time (time to appearance of negative curvature at the flame tip as seen in Fig. 5) decreases at the laser powers less than 12 W. Then, the volume of total burned gas at the start time of regime 2 is less than that of the lower laser powers cases, which causes low average temperatures and low acoustic frequancies. After the minimum at 12W, the transition time again increases and the ratio of burned gas at the start of regime 2 increases with increase in the laser power.

To elucidate the situation of the increases in the transition time and acoustic frequency at laser powers larger than 12W, we tried to count the temperature change along the center line by absorption of CO_2 laser. By using Beer`s law (A/A_0=exp($-acL$)) for the length of penetration of the laser power, where A is the energy after the absorption media and A_0 the energy before that. The a, c and L terms are the absorption coefficient (1.5 atm^{-1} cm^{-1}, C_2H_4), partial pressure (0.09 atm, C_2H_4) and the path length of the laser light respectively. With this, the penetration length and temperature distribution can be calculated considering energy conservation (A-A_0=cm△T, c: mixture`s heat capacity, m: mass of control volume, △T: temperature increase). The calculation result of the 18W condition is shown in figure 8. The maximum temperature is established right ahead of the flame front. The preheating effect ahead of the flame front enhances the local flame velocity non-linearly and increase the transition time to the concave structure. To verify this hypothesis, it is planned to investigate the changes in flame velocity depending on the laser power intensity by calculation further.

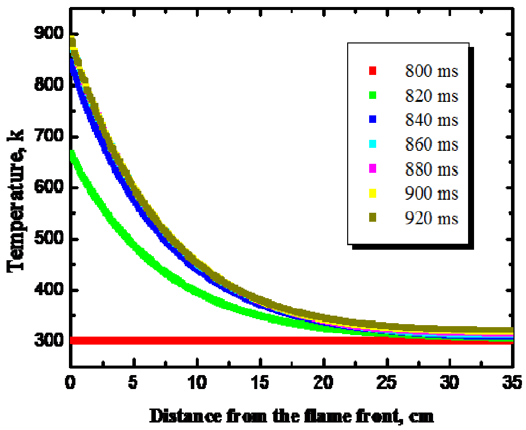

Figure 8. Calculated temperature distribution of unburned mixture with a laser power of 18W.

4 Summary

An artificial induction of the transition from propagating flat flames to turbulent flames in a combustion tube has been conducted by using a CO_2 laser method and an attempt was made to determine the threshold of the transition in terms of laser light intensity and supply time. The results may be summarized as follows:

(1) There is a minimum laser power (8W with 3.3mm beam diameter in this study) necessary to attain the transition. Below this power, flame tips do not grow to reach the secondary instability.

(2) The transition time is defined as the time of the first formation of a concave structure at the flame tip. The time with this definition corresponds well to the time taken to develop the turbulent motion because the structure is always followed by the immediate appearance of the secondary instability and the resulting turbulent motion.

(3) The transition time showed a minimum value at a laser power of 12 W. At lower and higher laser powers than this, the laser intensity results in longer times till the transition occurs. The mechanism of this dependence is still not satisfactorily explained, although a possible explanation is provided in the text.

Acknowledgement

This study was supported by a Grant-in-Aid for Scientific Research (KIBAN (B) #21360090) from MEXT Japan.

References

[1] Law C.K (2006). Combustion Physics. Cambridge, 396.

[2] Landau L. (1944). On the theory of slow combustion. Acta Phisicochi. URSS. 19:77.

[3] Clanet C. and Searby G. (1998). First Experimental study of the Darrieus-Landau Instability. Physical review letters. 80:3867.

[4] Rayleigh L. (1878). The explanation of certain acoustical phenomena. Nature. 18:319.

[5] Searby G. (1992). Acoustic Instability in Premixed Flames. Combustion Science and Technology. 81:221.

[6] Searby G. and Rochwerger D. (1991). A parametric acoustic instability in premixed flames. Journal of Fluid Mechanics. 231:529.

[7] Pelce P. and Rochwerger D. (1992). Vibratory instability of celluler flames propagating in tubes. Journal of Fluid Mechanics. 239:293.

[8] Park J. S., Fujita O., Nakamura Y., Ito H. (2011). Transition of Flat Flames to Turbulent Motion Induced by External Laser Irradiation. Proceedings of combustion institute. 33:1105.

[9] The national institute of standards and technology (NIST), available at < http://webbook.nist.gov/chemistry/>.